Available online at www.sciencedirect.com
SCIENCE DIRECT®
Microporous and Mesoporous Materials 78 (2005) 209–215
MICROPOROUS AND MESOPOROUS MATERIALS
www.elsevier.com/locate/micromeso

Chiral open-framework uranyl molybdates. 1. Topological diversity: synthesis and crystal structure of $[(C_2H_5)_2NH_2]_2[(UO_2)_4(MoO_4)_5(H_2O)](H_2O)$

Sergey V. Krivovichev [a,*], Christopher L. Cahill [b,c], Evgeniy V. Nazarchuk [a], Peter C. Burns [d], Th. Armbruster [e], Wulf Depmeier [f]

[a] *Department of Crystallography, St. Petersburg State University, University Emb. 7/9, 199034 St. Petersburg, Russia*
[b] *Department of Chemistry, The George Washington University, Washington, DC 20052, USA*
[c] *Geophysical Laboratory, Carnegie Insitution of Washington, Washington, DC 20015, USA*
[d] *Department of Civil Engineering and Geological Sciences, University of Notre Dame, 156 Fitzpatrick Hall, Notre Dame 46556 IN, USA*
[e] *Laboratorium für chemische and mineralogische Kristallographie, Universität Bern, Freiestrasse 3, CH-3102 Bern, Switzerland*
[f] *Institut für Geowissenschaften, Kiel Universität, Olshausenstrasse 40, D-24118 Kiel, Germany*

Received 5 April 2004; received in revised form 7 October 2004; accepted 8 October 2004
Available online 30 November 2004

Abstract

Crystals of a new framework uranyl molybdate, $[(C_2H_5)_2NH_2]_2[(UO_2)_4(MoO_4)_5(H_2O)](H_2O)$, were synthesized from a solution of $UO_2(CH_3COO)_2 \cdot 2H_2O$, MoO_3, diethylamine and HCl in H_2O at 220 °C. The structure was studied at −127 °C. The compound is hexagonal, space group $P6_522$, $a = 11.3612(13)$, $c = 52.698(8)$ Å, $V = 5890.7(13)$ Å^3, $Z = 3$. The structure has been refined to $R_1 = 0.050$ ($wR_2 = 0.100$; $S = 0.985$) on the basis of 3103 unique observed reflections. The structure consists of a three-dimensional framework of composition $[(UO_2)_4(MoO_4)_5(H_2O)]^{2-}$ that consists of UO_7 pentagonal bipyramids that share equatorial corners with MoO_4 tetrahedra. The framework contains a three-dimensional system of channels. The first system of channels is parallel to [0 0 1] and has the dimensions 7.0 × 7.0 Å, which result in a crystallographic free diameter (effective pore width) of 4.3 × 4.3 Å (based on an oxygen radius of 1.35 Å). Other channels run parallel to [1 0 0], [1 1 0] and [0 1 0] and have dimensions 5.2 × 7.1 Å (giving an effective pore width of 2.5 × 4.4 Å). One symmetrically unique $[(C_2H_5)_2NH_2]^+$ cation and H_2O molecule reside in the framework cavities. The channels parallel to [0 0 1] are chiral and are centered about a 6_5 screw axis. The uranyl framework with U:Mo = 4:5 in the structure of $[(C_2H_5)_2NH_2]_2[(UO_2)_4(MoO_4)_5(H_2O)](H_2O)$ represents the third known type of chiral uranyl molybdate framework. Its relationships to the frameworks with U:Mo = 5:7 and 6:7 can be understood in terms of fundamental chains that have related but yet different topological structure.

Keywords: Uranyl molybdates; Open framework; Crystal structure; Chiral; Nodal representation

1. Introduction

Uranium-based open-framework materials have attracted considerable attention due to their importance for radioactive waste management, uranium geochemistry and possible applications in ion-exchange, catalysis, etc. [1–5]. Among hexa-valent uranium oxysalts, uranyl molybdates show the greatest structural diversity due to

* Corresponding author. Address: Leopold-Franzens-Universität, Institut für Mineralogie und Petrographie, Innrain 52, 6020 Innsbruck, Austria.
E-mail address: skrivovi@mail.ru (S.V. Krivovichev).

1387-1811/$ - see front matter © 2004 Elsevier Inc. All rights reserved.
doi:10.1016/j.micromeso.2004.10.018

the high flexibility of U–O–Mo linkages and a wide range of topological possibilities [6–18]. Recently, we have described $(NH_4)_4[(UO_2)_5(MoO_4)_7](H_2O)$, a new material based upon an open framework of corner-linked UO_7 pentagonal bipyramids and MoO_4 tetrahedra [19]. It is noteworthy that the framework is chiral and at least one channel system of the framework is characterized by an internal helical structure. In this regard, the structure of $(NH_4)_4[(UO_2)_5(MoO_4)_7](H_2O)$ was found to be related to the structures of $M_2(UO_2)_6(MoO_4)_7(H_2O)_n$ (M = Sr, Mg; $n = 15$, 18) reported by Tabachenko et al. [20] and to the recently reported uranyl sulfate material $[NC_4H_{12}]_2[(UO_2)_6(H_2O)_2(SO_4)_7]$ [21]. However, analysis of the topology of interpolyhedral linkage by means of the graph theory demonstrated that the frameworks are different and cannot be transformed into another one without fundamental topological reconstruction [19].

In this series of papers, we further explore the structural chemistry of chiral framework uranyl molybdates. Herein we present results of hydrothermal synthesis and crystal structure determination of a new member of the family, $[(C_2H_5)_2NH_2]_2[(UO_2)_4(MoO_4)_5(H_2O)](H_2O)$, and discuss its relationships with other chiral open-framework uranyl molybdates.

2. Experimental

2.1. Synthesis

Crystals of $[(C_2H_5)_2NH_2]_2[(UO_2)_4(MoO_4)_5(H_2O)](H_2O)$ were synthesized from a solution of $UO_2(CH_3COO)_2 \cdot 2H_2O$ (0.1568 g), MoO_3 (0.0576 g), diethylamine (0.03 g) and HCl (0.053 g) in 5 ml of H_2O (with an approximate U:Mo:diethylamine:HCl:H_2O molar gel ratio of 4:4:7:15:2780). The solution was placed in a Teflon-lined Parr bomb and heated to 220 °C for 65 h, followed by cooling to ambient temperature. The crystals occur as aggregates of greenish-yellow transparent bipyramids up to 0.2 mm in maximum dimension.

It is noted that a material with the identical framework structure as that described herein may be synthesized under similar conditions using decane diamine in place of the ethylenediamine. As with the title compound however, characterization of the organic guest remained elusive and thus it is not certain if this larger template molecule remained intact.

2.2. Crystal-structure analysis

A single greenish-yellow bipyramid was mounted on a thin glass fiber for X-ray diffraction analysis. More than a hemisphere of X-ray diffraction data ($\theta_{max} = 34.44°$) were collected at room temperature using a Bruker SMART APEX CCD diffractometer with MoKα radiation located at the University of Notre Dame. The data were integrated and corrected for absorption using an empirical ellipsoidal model using the Bruker programs SAINT and XPREP. The compound was found to be hexagonal, $a = 11.4534(6)$, $c = 52.954(4)$ Å. The observed systematic absences were consistent with space groups $P6_122$ and $P6_522$. The structure was solved in space group $P6_522$ by direct methods and refined to $R_1 = 0.052$ on the basis of F^2 for all unique data using SHELXTL software (Flack parameter $x = 0.02(3)$). However, structure refinement from the room-temperature data did not allow location of the organic molecules within the framework cavities. Consequently, X-ray diffraction data was collected at −127 °C using a Bruker SMART 1K CCD diffractometer with MoKα radiation located at the University of Bern. The −127 °C data allowed deduction of the positions of protonated diethylamine molecules, although soft restraints on the geometry were necessary. The refinement of the structure resulted in disorder of one of the Mo atoms (see below). The final refinement converged to $R_1 = 0.050$, $wR_2 = 0.100$ and GoF = 0.985. The final model included anisotropic displacement parameters for U, Mo and O atoms with more-than-half occupancy, all atomic positional parameters, and isotropic-displacement parameters for N, C and H_2O groups. Further details of the data collection and refinement are given in Table 1 for the data collected at −127 °C, atomic coordinates are in Table 2, and selected bond lengths and angles are in Table 3.

2.3. X-ray powder-diffraction study

An X-ray powder-diffraction pattern of $[(C_2H_5)_2NH_2]_2[(UO_2)_4(MoO_4)_5(H_2O)](H_2O)$ was recorded at room temperature using a DRON-2 powder diffractometer and CuKα radiation ($\lambda = 1.54059$ Å). The unit-cell parameters refined from powder data using least-squares method on the basis of 40 reflections [$a = 11.4534(9)$, $c = 52.947(5)$ Å] are in agreement with those measured from single-crystal data.

2.4. High-temperature X-ray powder diffraction

High-temperature X-ray powder diffraction study was performed in the range of temperatures from 20 to 700 °C by means of a DRON-3 powder diffractometer equipped with a high-temperature KRV-1100 chamber. The phase is stable until 275 ± 10 °C, when the formation of a melting phase is observed. At 500 ± 10 °C, the loss of water and organic species is complete and UO_2MoO_4 crystallizes. The unit-cell dimensions show linear dependence versus temperature: $a(t) = 11.441 - 0.00047t$, $c(t) = 52.90 + 0.002t$ [Å], $V(t) = 5998 - 0.31t$ [Å^3]. The main thermal expansion coefficients are: $\alpha_{33} = 37.8$, $\alpha_{11} = 40.9$ and $\alpha_V = 51.7(\times 10^{-6}\,°C^{-1})$.

Table 1
Crystallographic data and refinement parameters for $[(C_2H_5)_2NH_2]_2$-$[(UO_2)_4(MoO_4)_5(H_2O)](H_2O)$ at −127 °C

a (Å)	11.3612(13)
c (Å)	52.698(8)
V (Å^3)	5890.7(13)
Space group	$P6_522$
F_{000}	5388
μ(cm^{-1})	180.61
Z	3
D_{calc} (g/cm^3)	3.47
Crystal size (mm)	0.12 × 0.10 × 0.06
Radiation	MoKα
Ref. for cell refinement	963
Absorption correction	Empirical
Ref. for abs. corr.	1689
Total Ref.	35458
Unique Ref.	4716
Unique $\lvert F_o\rvert \geqslant 4\sigma_F$	3103
R_1	0.050
wR_2	0.100
S	0.985

Note: $R_1 = \Sigma\|F_o| - |F_c\|/\Sigma|F_o|$; $wR_2 = \{\Sigma[w(F_o^2 - F_c^2)^2]/\Sigma[w(F_o^2)^2]\}^{1/2}$; $w = 1/[\sigma^2(F_o^2) + (aP^2) + bP]$, where $P = (F_o^2 + 2F_c^2)/3$; $s = \{\Sigma[w(F_o^2 - F_c^2)]/(n-p)\}^{1/2}$ where n is the number of reflections and p is the number of refined parameters.

3. Results

3.1. Cation coordination

The structure contains two symmetrically unique U^{6+} cations, each of which is strongly bonded to two oxygen atoms, giving nearly linear uranyl $(UO_2)^{2+}$ ions (Ur). Each uranyl ion is coordinated by five additional O atoms located at the equatorial vertices of pentagonal bipyramids that are capped by the O_{Ur} atoms. Bond lengths within the uranyl ions range from 1.71 to 1.77 Å, whereas the U–O bond lengths corresponding to the equatorial ligands range from 2.30 to 2.42 Å, which is typical for UO_7 polyhedra in uranyl oxysalts [22]. Each Mo^{6+} cation is tetrahedrally coordinated by four O atoms. Two of the four Mo positions, Mo(3) and Mo(3a) are partially occupied with site occupanies of 0.33 and 0.17, respectively. Each of these positions is also splitted into two half-populated sites. The nature of disorder is illustrated in Fig. 1. The crystal-chemical role of the $Mo(3)O_4$ and $Mo(3a)O_4$ tetrahedra is to link three adjacent UO_7 bipyramids (Fig. 1(a)). The Mo(3) and Mo(3a) atoms are bonded to the same three O

Table 2
Atomic coordinates and displacement parameters for $[(C_2H_5)_2NH_2]_2[(UO_2)_4(MoO_4)_5(H_2O)](H_2O)$ at −127 °C

Atom	x	y	z	U_{eq}	U_{11}	U_{22}	U_{33}	U_{23}	U_{13}	U_{12}
U(1)	0.53624(6)	0.05857(6)	0.05392(1)	0.0301(2)	0.0396(4)	0.0245(3)	0.0183(3)	−0.0025(3)	0.0020(3)	0.0101(3)
U(2)	0.10398(6)	−0.50784(7)	0.00546(1)	0.0383(2)	0.0332(4)	0.0485(4)	0.0255(3)	−0.0020(3)	0.0076(3)	0.0147(3)
Mo(1)	0.5426(1)	0.20550(14)	0.11834(2)	0.0257(3)	0.0282(8)	0.0271(8)	0.0181(7)	−0.0014(6)	0.0010(6)	0.0111(7)
Mo(2)	0.5070(2)	−0.23222(14)	0.00694(3)	0.0293(3)	0.0382(9)	0.0278(8)	0.0210(7)	−0.0017(6)	0.0021(7)	0.0160(7)
Mo(3)[a]	0.1952(4)	−0.2465(4)	0.06616(8)	0.0248(12)	0.027(2)	0.027(2)	0.016(2)	−0.0007(16)	−0.002(2)	0.010(2)
Mo(3a)[b]	0.2516(11)	−0.3027(11)	0.0678(2)	0.050[d]						
O(1)	0.4646(10)	0.1364(10)	0.08936(17)	0.026(2)	0.027(6)	0.028(6)	0.010(5)	−0.004(4)	0.003(5)	0.003(5)
O(2)	0.0735(13)	−0.3990(13)	−0.0119(2)	0.065(4)	0.051(8)	0.079(10)	0.050(9)	−0.038(7)	0.002(7)	0.022(8)
O(3)	0.4179(11)	0.0647(11)	0.0329(2)	0.041(3)	0.040(7)	0.033(7)	0.037(8)	0.005(6)	−0.001(5)	0.009(6)
O(4)	0.5649(10)	−0.1316(10)	−0.0202(2)	0.031(3)	0.028(6)	0.023(6)	0.032(7)	−0.006(5)	−0.009(5)	0.005(5)
O(5)	0.5108(12)	−0.1370(10)	0.0333(2)	0.043(3)	0.066(9)	0.030(7)	0.027(7)	−0.007(5)	0.001(6)	0.019(7)
O(6)	0.6521(11)	0.0509(11)	0.0751(2)	0.043(3)	0.050(8)	0.040(7)	0.028(7)	0.009(6)	−0.003(6)	0.014(6)
O(7)	0.7026(9)	0.3426(10)	0.1117(2)	0.030(3)	0.010(5)	0.032(6)	0.032(6)	0.006(5)	−0.006(4)	−0.002(5)
O(8)	0.4455(11)	0.2605(12)	0.1342(2)	0.043(3)	0.029(7)	0.047(7)	0.053(8)	−0.022(6)	−0.005(6)	0.018(6)
O(9)	0.3571(12)	−0.1283(11)	0.0726(2)	0.048(3)	0.050(8)	0.024(7)	0.040(7)	0.004(5)	0.014(6)	−0.003(6)
O(10)	0.6080(14)	−0.3060(12)	0.0137(2)	0.051(4)	0.094(10)	0.064(8)	0.023(7)	−0.009(6)	−0.023(6)	0.062(8)
O(11)	0.3358(12)	−0.3565(11)	0.0018(2)	0.045(3)	0.047(7)	0.033(6)	0.040(8)	−0.012(6)	0.016(6)	0.008(6)
O(12)	0.5620(12)	0.0850(11)	0.1346(2)	0.051(3)	0.069(9)	0.041(7)	0.044(8)	0.009(6)	0.002(6)	0.028(7)
O(13)	0.1367(12)	−0.6202(13)	0.0230(2)	0.050(3)	0.037(7)	0.062(9)	0.044(8)	0.008(6)	0.001(6)	0.020(7)
O(14)	0.1831(15)	−0.3509(14)	0.0408(2)	0.078(5)	0.095(11)	0.073(10)	0.032(8)	−0.022(7)	0.018(8)	0.017(9)
O(15)[a]	0.109(5)	−0.157(5)	0.0590(10)	0.100[d]						
O(15a)[b]	0.361(10)	−0.368(12)	0.0720(17)	0.100[d]						
H_2O(16)[c]	0.058(4)	−0.113(4)	0.0003(9)	0.150[d]						
N	0.946(3)	0.165(3)	−0.0725(5)	0.150[d]						
C(1)	0.005(3)	−0.259(3)	−0.0733(6)	0.150[d]						
C(2)	−0.027(4)	−0.405(3)	−0.0735(7)	0.150[d]						
C(3)	0.027(3)	0.155(4)	−0.0515(5)	0.150[d]						
C(4)	0.016(3)	0.071(3)	−0.0280(6)	0.150[d]						

[a] s.o.f. (site-occupation factor) = 0.33.
[b] s.o.f. = 0.17.
[c] s.o.f. = 0.50.
[d] Fixed during refinement.

Table 3
Selected bond lengths (Å) in the structure of $[(C_2H_5)_2NH_2]_2[(UO_2)_4(MoO_4)_5(H_2O)](H_2O)$ at −127 °C

U(1)–O(6)	1.76(1)	Mo(2)–O(4)	1.74(1)
U(1)–O(3)	1.77(1)	Mo(2)–O(5)	1.75(1)
U(1)–O(9)	2.30(1)	Mo(2)–O(10)	1.76(1)
U(1)–O(7)	2.350(9)	Mo(2)–O(11)	1.76(1)
U(1)–O(5)	2.36(1)	⟨Mo(2)–O⟩	1.75
U(1)–O(4)	2.38(1)		
U(1)–O(1)	2.38(9)	Mo(3)–O(9)	1.68(1)
⟨U(1)–O_{Ur}⟩	1.77	Mo(3)–O(14)	1.74(1)
⟨U(1)–O_{eq}⟩	2.35	Mo(3)–O(15)	1.77(1)
		Mo(3)–O(9)	1.83(1)
U(2)–O(2)	1.71(2)	⟨Mo(3)–O⟩	1.76
U(2)–O(13)	1.76(1)		
U(2)–O(11)	2.32(1)	Mo(3a)–O(14)	1.58(2)
U(2)–O(12)	2.37(1)	Mo(3a)–O(9)	1.75(1)
U(2)–O(8)	2.37(1)	Mo(3a)–O(15a)	1.76(2)
U(2)–O(10)	2.36(1)	Mo(3a)–O(9)	1.84(2)
U(2)–O(14)	2.42(1)	⟨Mo(3a)–O⟩	1.73
⟨U(2)–O_{Ur}⟩	1.74		
⟨U(2)–O_{eq}⟩	2.37	N–C(1)	1.47(1)
		N–C(3)	1.48(1)
Mo(1)–O(12)	1.72(1)	C(1)–C(2)	1.51(1)
Mo(1)–O8	1.73(1)	C(3)–C(4)	1.53(1)
Mo(1)–O7	1.739(9)		
Mo(1)–O1	1.743(9)		
⟨Mo(1)–O⟩	1.73		

atoms, O(9), O(9) and O(14). The fourth O atoms of the $Mo(3)O_4$ and $Mo(3a)O_4$ tetrahedra are the O(15) and O(15a) atoms. Thus, there are four partially occupied Mo sites (with total occupancy of 1.00) and only one can be populated locally. If the Mo(3) site is populated (Fig. 1(b)), it is bonded to two O(9) sites, one O(15) site and one O(14) site. In this scenario, the O(14) site on the other side relative to the U(1)–U(1) line is populated by H_2O. The same holds for the case where the Mo(3a) site is occupied (Fig. 1(c)). Therefore, the overall occupation of the O(14) position is $O_{0.50}(H_2O)_{0.50}$. It is noteworthy that the U(2)–O(14) distance of 2.42 Å is typical for the U–H_2O bond-lengths in uranyl molybdates [10]. The Mo–O–U angles range from 129.8° to 165.6°, reflecting the substantial flexibility of Mo–O–U connections.

Bond-valence sums for the cation positions calculated using bond-valence parameters for the U^{6+}–O bonds taken from [22] and for the Mo^{6+}–O bonds taken from [23] are 6.20, 6.34, 6.40, 6.08, 6.10 and 6.64 valence units (v.u.) for the U(1), U(2), Mo(1), Mo(2), Mo(3) and Mo(3a) cations, respectively. The deviations from the ideal values of 6 v.u. can be explained by the fact that the bond-valence parameters used were determined for the room-temperature conditions and do not account for thermal contraction of chemical bonds. In addition, the presence of disorder at the Mo(3) and Mo(3a) sites results in significant errors in the Mo–O bond lengths, as they correspond to the averages of occupied and unoccupied tetrahedra.

3.2. Structure description

The structure of $[(C_2H_5)_2NH_2]_2[(UO_2)_4(MoO_4)_5(H_2O)](H_2O)$ is a three-dimensional framework of composition $[(UO_2)_4(MoO_4)_5(H_2O)]^{2-}$ that consists of UO_7 pentagonal bipyramids that share equatorial corners with MoO_4 tetrahedra (Fig. 2). The framework contains a three-dimensional system of channels. The first system of channels is parallel to [0 0 1] and has the dimensions 7.0 × 7.0 Å, which result in a crystallographic free diameter (effective pore width) of 4.3 × 4.3 Å (based on an oxygen radius of 1.35 Å). Other channels run parallel to [1 0 0], [1 1 0] and [0 1 0] and have dimensions

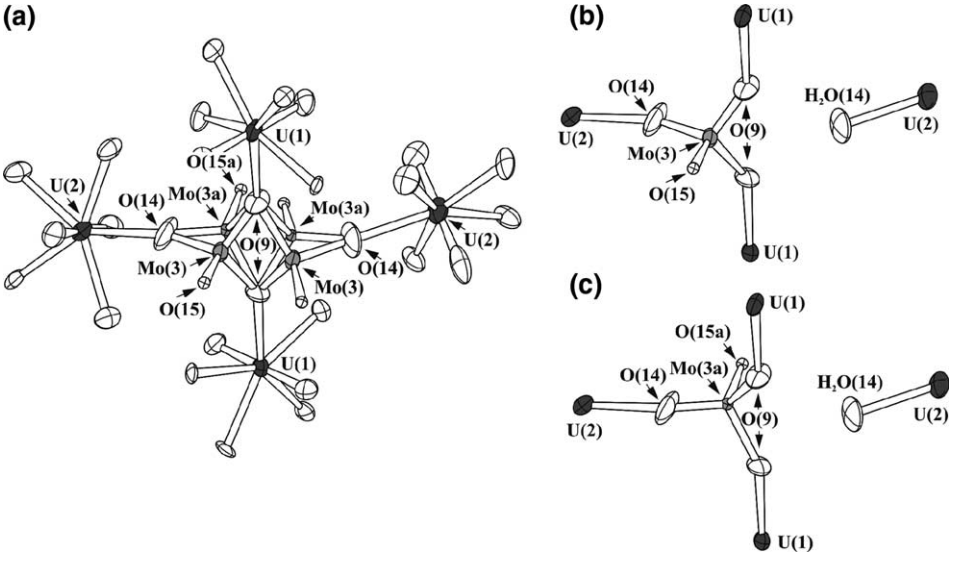

Fig. 1. Disorder of Mo(3) and Mo(3a) sites in the structure of $[(C_2H_5)_2NH_2]_2[(UO_2)_4(MoO_4)_5(H_2O)](H_2O)$: configuration with four disordered Mo sites with sum occupancy of 1 (a); configuration with one Mo(3) site occupied (b); configuration with one Mo(3a) site occupied (c).

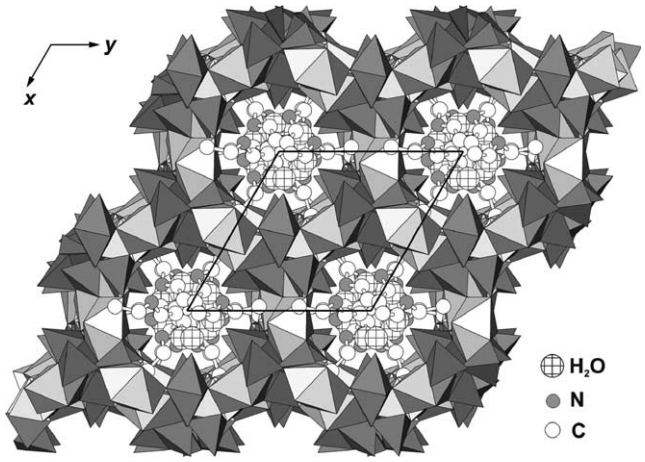

Fig. 2. The structure of $[(C_2H_5)_2NH_2]_2[(UO_2)_4(MoO_4)_5(H_2O)](H_2O)$ projected along the *c* axis.

5.2×7.1 Å (giving an effective pore width of 2.5×4.4 Å). One symmetrically unique $[(C_2H_5)_2NH_2]^+$ cation and $H_2O(16)$ molecules are present in the framework cavities.

4. Discussion

The $[(UO_2)_4(MoO_4)_5(H_2O)]^{2-}$ framework in the structure of $[(C_2H_5)_2NH_2]_2[(UO_2)_4(MoO_4)_5(H_2O)](H_2O)$ is very complex. Its topological structure may be described using a nodal representation that is very suitable for the description of heteropolyhedral units in uranyl molybdates, chromates, sulfates, etc. [16,17,24–26]. Each node corresponds to a UO_7 bipyramid (black) or a MoO_4 tetrahedron (white). Nodes are shown connected if the polyhedra share a common vertex (O atom). The uranyl molybdate framework is a three dimensional infinite net, where all black vertices are 5-connected and all white vertices are either 3- or 4-connected.

By analogy with the framework in the structure of $(NH_4)_4[(UO_2)_5(MoO_4)_7](H_2O)$, the uranyl molybdate framework in the structure of $[(C_2H_5)_2NH_2]_2[(UO_2)_4(MoO_4)_5(H_2O)](H_2O)$ can be described in terms of either fundamental chains or tubular building units. The concept of the fundamental chain was proposed by Liebau [27] for the description of complex silicate structures. Sheets and frameworks of polyhedra can be regarded as based upon appropriately chosen chains of polyhedra. The fundamental chain corresponding to the uranyl molybdate framework in the structure of $[(C_2H_5)_2NH_2]_2[(UO_2)_4(MoO_4)_5(H_2O)](H_2O)$ is shown in Fig. 3(a); its nodal representation is given in Fig. 3(b). The chain extends along [0 0 1] and represents a sequence of 3- and 4-connected MoO_4 tetrahedra (white vertices) linked through one, two or three UO_7 pentagonal bipyramids (black vertices). Fig. 3(c) and (d) provide nodal representations of fundamental chains present in the structures of $(NH_4)_4[(UO_2)_5(MoO_4)_7](H_2O)$ [19] and $M_2(UO_2)_6(MoO_4)_7(H_2O)_n$ (M = Sr,

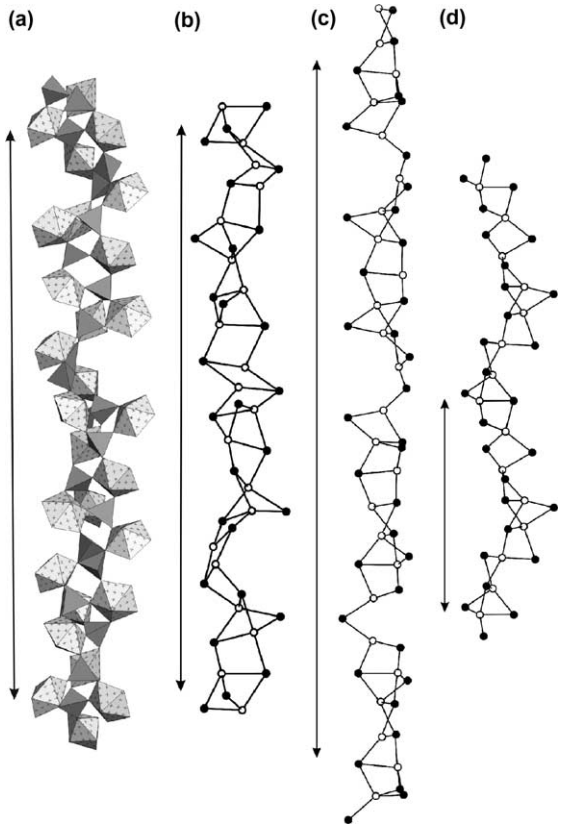

Fig. 3. Fundamental chain of UO_7 and MoO_4 polyhedra in the structure of $[(C_2H_5)_2NH_2]_2[(UO_2)_4(MoO_4)_5(H_2O)](H_2O)$ (a) and its nodal representation (b); nodal representations of fundamental chains in the structures of $(NH_4)_4[(UO_2)_5(MoO_4)_7](H_2O)$ (c) and $M[(UO_2)_6(MoO_4)_7](H_2O)_n$ (M = Sr, Mg) (d). Legend: UO_7 polyhedra = black circles; fully-occupied MoO_4 tetrahedra = white circles; half-occupied MoO_4 tetrahedra = grey circles.

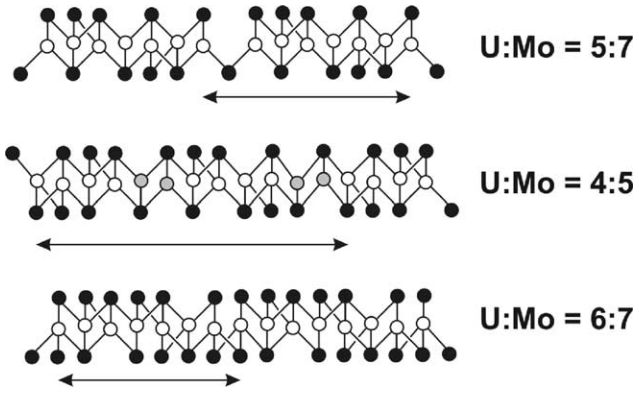

Fig. 4. Black-and-white graphs isomorphous to the nodal representations of fundamental chains shown in Fig. 3. Note that the graphs shown cannot be transformed one into another without significant topological reconstruction. Legend: UO_7 polyhedra = black circles; MoO_4 tetrahedra = white circles.

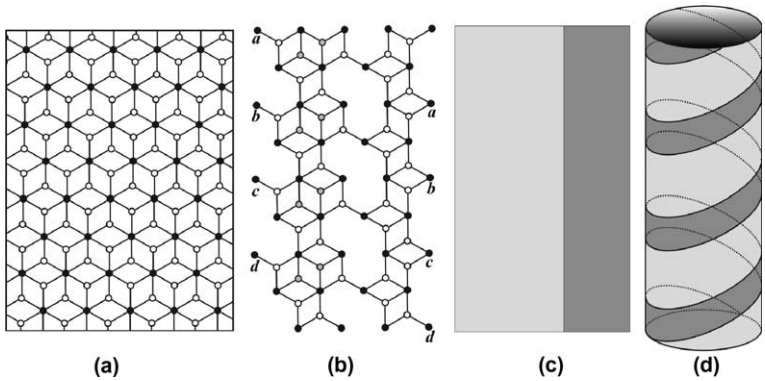

Fig. 5. Construction of a tubular unit corresponding to the interior of channels along [0 0 1] in the structure of $[(C_2H_5)_2NH_2]_2[(UO_2)_4(MoO_4)_5(H_2O)](H_2O)$: (a) black-and-white {3.6.3.6} graph with 3-connected white and 6-connected black nodes; (b) tape extracted from the graph shown in (a); (c) tape shown in (b) consists of two narrower chains; (d) folding and linkage of tapes shown in (b) and joining of their ***a–a***, ***b–b***, ***c–c***, ***d–d***, etc. nodes produces chiral tubular unit with a helical structure.

Mg; $n = 15$, 18) [20], respectively. The black-and-white graphs depicted in Fig. 3(b)–(d) can be further reduced to the simplified isomorphic graphs shown in Fig. 4. This reduction preserves all topological linkages between the polyhedra. Topological analysis of the connectivities of the graphs shown in Fig. 4 demonstrate that they cannot be transformed into another one without significant topological reconstruction. Thus, the fundamental chains that form bases for the chiral uranyl molybdate frameworks with U:Mo = 5:7, 4:5 and 6:7 are topologically different, though closely related.

The internal topological structure of one dimensional channels parallel to [0 0 1] can also be described using nodal representation. The channel is viewed as a tubular building unit, with the topological construction illustrated in Fig. 5. The basis for the unit is a two dimensional black-and-white net {**3.6.3.6**} consisting of 3-connected white and 6-connected black nodes (Fig. 5(a)). This net is the basis of a large number of heteropolyhedral units as discussed in [28]. The net is cut into the wide tapes shown in Fig. 5(b). The tape can be considered as consisting of two chains as depicted in Fig. 5(b) and (c). To produce the tubular unit, the tape should be folded around a cylinder and joined at its corresponding points ***a–a***, ***b–b***, ***c–c***, ***d–d***, etc. as it is shown in Fig. 5(b). The result is the double-helix tubular unit in which both chains form a spiral with axes parallel to [0 0 1] (Fig. 5(d)). Note that chirality of the unit is in agreement with the chiral space group $P6_522$.

5. Conclusions

Here we have described a novel type of chiral uranyl molybdate framework that is related, yet distinct from the frameworks observed in the structures of $(NH_4)_4[(UO_2)_5(MoO_4)_7](H_2O)$ [19] and $M[(UO_2)_6(MoO_4)_7](H_2O)_n$ (M = Sr, Mg) [20]. There are thus three topological types of chiral uranyl molybdate frameworks known to date. These frameworks differ in their U:Mo ratio of 5:7, 4:5 and 6:7. Topological relationships between the frameworks can be described using nodal representation. In agreement with our previous studies concerning the crystal chemistry of uranyl molybdates [6–20], the current study further demonstrates the structural complexity and variability observed in this interesting class of compounds. Here, flexible U–O–Mo linkages give rise to the appearance of new framework topology. In the next contributions, we shall discuss flexibility of uranyl molybdate frameworks as a function of composition and geometrical shape of extra-framework species and as a function of temperature.

Acknowledgment

This research was supported by the Environmental Management Sciences Program of the United States Department of Energy (Grant DE-FG07-97ER14820). S.V.K. thanks the Alexander von Humboldt Foundation and the Swiss National Foundation for financial support during his stay at Bern.

References

[1] Y. Li, C.L. Cahill, P.C. Burns, Chem. Mater. 13 (2001) 4026.
[2] X. Wang, J. Huang, A.J. Jacobson, J. Am. Chem. Soc. 124 (2002) 15190.
[3] A.J. Locock, P.C. Burns, J. Solid State Chem. 167 (2002) 226.
[4] R.E. Sykora, T.E. Albrecht-Schmitt, Inorg. Chem. 42 (2003) 2179.
[5] T.A. Sullens, R.A. Jensen, T.Y. Shvareva, T.E. Albrecht-Schmitt, J. Am. Chem. Soc. 126 (2004) 2676.
[6] V.N. Khrustalev, G.B. Andreev, M.Yu. Antipin, A.M. Fedoseev, N.A. Budantseva, I.B. Shirokova, Russ. J. Inorg. Chem. 45 (2000) 1845.

[7] P.S. Halasyamani, R.J. Francis, S.M. Walker, D. O'Hare, Inorg. Chem. 38 (1999) 271.
[8] S.V. Krivovichev, P.C. Burns, Can. Mineral. 38 (2000) 847.
[9] S.V. Krivovichev, P.C. Burns, Can. Mineral. 39 (2001) 197.
[10] S.V. Krivovichev, P.C. Burns, Can. Mineral. 39 (2001) 207.
[11] S.V. Krivovichev, P.C. Burns, Can. Mineral. 40 (2002) 201.
[12] S.V. Krivovichev, P.C. Burns, J. Solid State Chem. 168 (2002) 245.
[13] S.V. Krivovichev, P.C. Burns, Inorg. Chem. 41 (2002) 4108.
[14] S.V. Krivovichev, P.C. Burns, Can. Mineral. 40 (2002) 1571.
[15] S.V. Krivovichev, P.C. Burns, Solid State Sci. 5 (2003) 481.
[16] S.V. Krivovichev, P.C. Burns, J. Solid State Chem. 170 (2003) 106.
[17] S.V. Krivovichev, C.L. Cahill, P.C. Burns, Inorg. Chem. 41 (2002) 34.
[18] S. Obbade, S. Yagoubi, C. Dion, M. Saadi, F. Abraham, J. Solid State Chem. 174 (2003) 19.
[19] S.V. Krivovichev, C.L. Cahill, P.C. Burns, Inorg. Chem. 42 (2003) 2459.
[20] V.V. Tabachenko, L.M. Kovba, V.N. Serezhkin, Koord. Khim. 10 (1984) 558.
[21] M. Doran, A.J. Norquist, D. O'Hare, Chem. Commun. (2002) 2946.
[22] P.C. Burns, F.C. Hawthorne, R.C. Ewing, Can. Mineral. 35 (1997) 1551.
[23] I.D. Brown, The Chemical Bond in Inorganic Chemistry. The Bond Valence Model, Oxford University Press, New York, 2002.
[24] S.V. Krivovichev, P.C. Burns, Z. Kristallogr. 218 (2003) 568.
[25] S.V. Krivovichev, P.C. Burns, Z. Kristallogr. 218 (2003) 683.
[26] S.V. Krivovichev, P.C. Burns, Z. Kristallogr. 218 (2003) 725.
[27] F. Liebau, Structural Chemistry of Silicates. Structure, Bonding and Classification, Springer, Berlin, 1985.
[28] S.V. Krivovichev, Crystallogr. Rev. 10 (2004) 185.